

IN VIVO EXPOSURE OF MICE SPLEEN TO MAGNETITE NANOPARTICLES ENCAPSULATED IN PHOSPHOLIPID POLYMERIC MICELLES; AN OXIDATIVE STRESS AND STRUCTURAL APPROACH

I. M. POPESCU^a, L. O. CINTEZA^b, A. HERMENEAN^{c,d}, A. DINISCHIOTU^{a*}

^a*Department of Biochemistry and Molecular Biology, Faculty of Biology, University of Bucharest, 91-95 Splaiul Independentei, 050095 Bucharest, Romania*

^b*Department of Physical Chemistry, Faculty of Chemistry, University of Bucharest, 4-12 Regina Elisabeta, 030018 Bucharest, Romania*

^c*Department of Experimental and Applied Biology, Institute of Life Sciences, Vasile Goldis Western University of Arad, 86 Rebreanu Street, 310414 Arad, Romania*

^d*Department of Histology, Faculty of Medicine, Pharmacy and Dentistry, Vasile Goldis Western University of Arad, 86 Rebreanu Street, 310414 Arad, Romania*

Magnetic nanoparticles (MNP) are potential agents for biomedical applications. In this study, we analysed some biochemical and structural changes in the spleen of mice exposed to 5 and 15mg/kg body weight of phospholipid polymeric micelles loaded with MNP, at 1, 2, 3, 7 and 14 days post-exposure. The spleens displayed progressive structural alterations and maximum iron deposition after 3 days, with changes being more apparent for higher doses. The biochemical responses to MNP exposure preceded the structural changes observed. Furthermore, while malondialdehyde (MDA) concentrations increased 1 day post-exposure by 26% and 28%, for the 5 and 15mg Fe/kg doses, its levels reverted to control ones after 3 days. The reduced glutathione (GSH) concentration showed an initial increase by 33% for the lower dose and 23% for the higher one after 1 day followed by a decrease near the control level on the third day of exposure for both doses. Advanced oxidation protein products (AOPP) level followed the same pattern as the GSH one. After 1 week of exposure, the morphological and biochemical changes observed were attenuated. Taken together, our data suggest that these phospholipid polymeric micelles loaded with MNP could be used as contrast agents, with further investigations being required for their safety assessment.

(Received June 4, 2015; Accepted August 3, 2015)

Keywords: MNP; Micelles; Spleen; Oxidative stress; Histological alteration

1. Introduction

In the last few years, nanoscience, nanotechnology and nanomedicine have seen many developments being made that have resulted in creating new types of magnetic iron oxide nanoparticles (MNP) [1,2]. The properties and numerous formulations developed in time make MNP suitable for many biomedical applications; to be more specific, these nanoparticles can function as contrast enhancement agents for magnetic resonance imaging (MRI - a non-invasive imaging method) due to their capability to alter the relaxation times of the tissues in which they are present [3], as mediators for hyperthermia treatments, as magnetic guidance for targeted drug delivery [4,5], as well as for cell tracking, biomolecular detection and blood pooling [6]. Also, they can be used for biosensors generation, rapid separation in the environmental biology and concentration tracing of specific targets, such as bacteria and proteins [7].

* Corresponding author: anca.dinischiotu@bio.unibuc.ro

MNP are widely used for medical purposes, such as: diagnosis, treatment and theranostics [8]. One of the concerns regarding the use of MNP is the way in which they interact with each other, with living organisms as well as the modality of their processing [1].

MNP are generally composed of Fe_3O_4 and/or $\gamma\text{-Fe}_2\text{O}_3$ and coated by desirable surface modifications which improve stability, prevent aggregation, diminish toxicity in physiological conditions and create the premises for specific targeting [9].

Previous studies have demonstrated that there could be a correlation between the chemical composition of the coating material, nanoparticles (NP), distribution and biocompatibility. To be more specific, it was observed that poloxamers coating facilitated the accumulation of NP in the sinusoidal bone marrow endothelium [10], whereas NP coated with Tween 80 (a non-ionic surfactant) were found in brain tissue [11] and MNP coated with starch appeared to be localized in the lymph nodes [12]. In addition, MNP with polyethylene glycol coating presented an excellent stability in various physiological solutions [13], while polymeric micelles carrying lipid entities conferred to MNP an appropriate hydrophobicity that helped maintain a good biocompatibility, i.e. low toxicity and immunological reactions [14].

MNP can be administered intravenously and also intragastrically [4]. It is assumed that when injected intravenously, the MNP undergo a series of transformations in order to be cleared from the body, with the reticuloendothelial system (liver, spleen and lymph nodes) being an important player in this process [15].

The aim of our study was to evaluate the biochemical and structural changes registered in the spleen of mice exposed to two different doses of modified phospholipid 1,2 – Distearoyl – sn – glycerol – 3 – phosphoethanolamine – N – methoxy (poly(ethylene glycol)) – 2000] (ammonium salt) (DSPE -PEG) micelles loaded with MNP.

2. Experimental

2.1. Materials

Modified phospholipid 1,2 – Distearoyl – sn – glycerol – 3 – phosphoethanolamine – N – methoxy (poly(ethylene glycol)) – 2000] (ammonium salt) (DSPE -PEG) from Avanti Polar Lipids was used as polymeric material for micelle preparation.

The substances Tris, EDTA, bovine serum albumin (BSA), chloramine-T, potassium iodide (KI), MDA standard, thiobarbituric acid (TBA) and solutions of iron(III) acetylacetonate ($\text{Fe}(\text{acac})_3$), 1,2 – hexadecanediol (90%), oleic acid (90%), oleylamine (70%), phenyl ether (99%), HCl, Folin-Ciocalteu phenol reagent, acetic acid, sodium chloride together with the Glutathione Assay Kit were purchased from Sigma-Aldrich Corporation.

Paraformaldehyde, paraffin, hematoxylin & eosin were purchased from Bio-Optica (Italy) and Perls staining kit from Titolchimica (Italy).

2.2. Synthesis of Fe_3O_4 MNP

The hydrophobic magnetic nanoparticles were synthesized using a previously reported method, with minor modifications [16].

In a typical synthesis, small magnetic nanoparticles (around 8 nm) were obtained by mixing together $\text{Fe}(\text{acac})_3$ (2 mmol), hexadecanediol (10 mmoles), oleic acid (6 mmoles) and oleylamine (6 mmoles) in phenyl ether (30 mL), under vigorous stirring, in a current of nitrogen. The mixture was heated to 265°C for 90 minutes in order to use the magnetic nanoparticles as seeds. After adding ethanol, the precipitated Fe_3O_4 nanoparticles were collected by centrifugation, and resuspended in hexane. These nanoparticles were presumed to grow larger in size in the $\text{Fe}(\text{acac})_3$ precursors solution according to the method of Sun et al [17].

The obtained magnetic NP were again precipitated in ethanol, separated by centrifugation and dispersed in chloroform in the presence of oleic acid.

2.3. Preparation of polymeric micelles loaded with MNP

The preparation of micelles with magnetic nanoparticles was performed using the standard thin-film hydration method followed by sonication. Briefly, the phospholipid polymeric derivative

DSPE - PEG was dissolved in chloroform with a certain amount of hydrophobically modified magnetic nanoparticles. The solvent was then evaporated under reduced pressure to produce a thin film onto the walls of the vial. The resulted mixed film was hydrated in distilled water or PBS to obtain the final concentrations of polymer at 20 mg/mL and magnetic nanoparticles at 1000 µg/mL. The micellar dispersion was sonicated for 2 minutes and filtered through a Millex filter (0.22-µm-diameter) for sterilization and removal of larger aggregates.

2.4. Characterization of polymeric micelles loaded with MNP

The dimension and zeta potential of the nanoparticles and micelles were measured using a Zetasizer Nano-ZS90 (Malvern Instruments). The particle size was determined by Dynamic Light Scattering (DLS), and the zeta potential was calculated by Laser Doppler Velocimetry (LDV). For both measurements the solvent was distilled water.

2.5. Animals and experimental design

For the *in vivo* study CD1 mice of both sexes, weighing between 20-30 g, were kept in normal feeding and watering conditions in IVC cages with controlled atmosphere-temperature, humidity and lighting. All animal care and study protocols complied with the guidelines of the Animal Facility of Vasile Goldis Western University of Arad and were approved by the Institutional Ethics Committee. During the experiments, the mice were processed according to the international ethical guidelines for the care of laboratory animals.

A number of 105 mice were randomly divided into 5 animal groups (of 21 individuals each) and then those were subdivided into three subgroups of 7 individuals each. The mice from the subgroups were then intravenously injected into the tail veins with a suspension of DSPE-PEG micelles loaded with MNP: the mice of 5 control subgroups were injected with a solution of 0.7% sodium chloride (n=7 mice / subgroup), and the other 10 subgroups were treated with two different concentrations of the suspension, 5 with a 5 mg Fe/kg body weight dose and the other 5 with a 15 mg Fe/kg body weight dose (n=7 mice / subgroup, for each dose).

The 5 groups of mice (each split into the 3 subgroups previously mentioned of n=7 mice: a control subgroup, a 5 mg Fe/kg body weight dose subgroup and a 15 mg Fe/kg body weight dose subgroup) were then sacrificed one by one at indicated time points, 1, 2, 3, 7 and 14 days and halves of all 105 spleens were excised and cryopreserved at -80°C for biochemical analyses. The rest of them were used for histological studies.

2.6. Biochemical analyses

2.6.1. Total protein extracts preparation

Total protein extracts were obtained from the previously cryopreserved spleens using a 0.1 M Tris-HCl/5 mM EDTA buffer, pH 7.4. A quantity of 0.1 g of each organ was carefully weighed and 1 mL of buffer was added. Then, the samples were homogenized on ice (Hielscher Ultrasonic processor UP50H) three times for 30 seconds. After 1 hour at 4°C they were centrifuged at 10000 rpm, 4°C for 30 minutes. The supernatants were then collected in order to analyse the level of some biomarkers of oxidative stress such as: AOPP, MDA and GSH.

The total protein concentration was assayed according to Lowry's method [18] using BSA as a standard.

2.6.2. Determination of MDA concentration.

The measurement of MDA, a thiobarbituric reacting substance that is used as a marker of lipid peroxidation, was performed according to a method described by Del Rio, 2003 [19], using a fluorescence spectrophotometer FP-6300 JASCO. A calibration curve, based on a 1 µM MDA standard solution was used. A volume of 200 µL total protein extracts of each sample, accordingly diluted, was mixed and incubated with 700 µL 0.1 N HCl for 20 minutes at room temperature. After this step, 900 µL of 0.025 M TBA were added, and another incubation at 37°C for 65 minutes occurred. Data from the fluorescence measurements ($\lambda_{ex}=520$ nm, $\lambda_{em}=549$ nm) of the MDA-TBA adducts were extrapolated on the calibration curve and expressed as relative fluorescence units (RFU), converted and calculated as nmoles/mg protein.

2.6.3. Determination of GSH concentration

The GSH concentration was determined using the Glutathione Assay Kit (Sigma-Aldrich, CS0260) according to the manufacturer's instructions. The total protein extracts were deproteinized with an equal volume of 5% sulfosalicylic acid and centrifuged at 10000 rpm for 30 minutes at 4°C. A volume of 10 µL of each supernatant was placed on a 96-well microtiter plate (Falcon Tissue Culture Plate, Becton Dickinson Labware) and then 150 µL of working mixture (8 mL of 100 mM potassium phosphate buffer, pH 7.0, with 1 mM EDTA – Assay Buffer and 228 µL of 1.5 mg/mL 5,5'-dithiobis-(2-nitro benzoic acid) (DTNB)) were added. After 5 minutes at room temperature the absorbance of the reaction mixture was read spectrophotometrically at a wavelength of 412 nm using a multiplate reader Genius TECAN and expressed in nmoles/mg protein.

2.6.4. Biochemical analysis of AOPP

AOPP levels were measured spectrophotometrically, according to the method described by Witko-Sarsat et al. [20], at 340 nm (Multiplate reader Genius TECAN), using a chloramine-T standard curve. A volume of 200 µL of total protein extract of each sample was diluted appropriately in 0.1 M Tris-HCl /5 mM EDTA solution, pH 7.4 and pipetted in a 96-well microtiter plate (Falcon Tissue Culture Plate, Becton Dickinson Labware) along with 10 µL of 1.16 M KI and 20 µL glacial acetic acid. The absorbance was immediately read and the concentration of AOPP was expressed as chloramine –T equivalent units in µmoles/L.

2.7. Histopathology

Spleen specimens were fixed in 4% paraformaldehyde and embedded in paraffin blocks. Sections (5 µm) were deparaffinized, rehydrated and stained with hematoxylin & eosin (HE).

Prussian blue staining was performed using a Perls staining kit (Titolchimica, Italy). This method for ferric iron staining is based on the reaction between potassium ferrocyanide and ferric ions in order to form a coloured salt of Prussian Blue. Deparaffinized slides were washed and immersed for 20 minutes in a mix solution of reagents A and B (potassium ferrocyanide solution, respectively acid activation buffer), followed by incubation with reagent C (carmalum according to Mayer).

For both staining types, dehydrated and cleared slides were mounted and examined under a light microscope (Olympus BX43, Hamburg, Germany).

2.8. Data analysis

Data were analysed using GraphPad Prism software (Version 6, Inc., La Jolla, CA 92037 USA) and expressed as mean values ± SD (n=7 mice / subgroup of individuals). The differences between groups were evaluated by two-way ANOVA followed by a post-hoc Bonferroni test. Statistical significance was assigned as probability value (p) of less than 0.05.

3. Results

The loading of the DSPE-PEG micelles with magnetic material was achieved during the preparation of the micelles. The size and the surface potential of the micelles and Fe₃O₄ nanoparticles are shown in Table 1.

Table 1. Size and zeta potential of the MNP and polymeric micelles used in this work

Sample	Size (nm)	Zeta potential (mV)
Pristine Fe ₃ O ₄ nanoparticles	13.8	-
DSPE-PEG micelles	15.8	-28.3

DSPE-PEG micelles loaded with magnetic NP

| 22.6

| -26.8

3.1. MNP characterization

Hydrophobically modified MNP, with oleic acid as a coating material were prepared, in order to be encapsulated in the core of the polymeric micelles.

The magnetic nanoparticles obtained were rather monodispersed (polydispersity index 0.098) with the average size of 13.8 nm and a concentration of 12.5 mg Fe/mL of suspension.

The micelles prepared from phospholipid polymeric derivative DSPE-PEG exhibited dimensions in the range 12-18 nm, that were according to the relevant literature[21].

The presence of the MNP encapsulated inside the core of the micelles led to an increase in the micelle size, while the surface potential remained practically unchanged.

The stability of the magnetic micelles was evaluated by measuring the variation of the size (using the DLS method) during storage at 15°C, protected from light. The dispersion was stable, without visible appearance of solid magnetic precipitate or variation of the micelle size for 2 months. Nevertheless, the DSPE-PEG micelles loaded with MNP were used in the experiment within two weeks from preparation.

3.2. MNP uptake and histological changes

The histological photomicrographs of the spleen sections are shown in Figure 1. Tissue sections of the control showed normal structure of the red and white pulp, for all intervals. Follicles in the white pulp were well organized with distinct marginal zones and germinal centres. The morphology of the spleen progressively changed with exposure time, with a maximum after 3 days and an attenuation at 7 day post-administration. The 15 mg Fe/kg body weight dose induced more severe alterations, which consisted in the atrophy of the splenic white pulp follicles, decrease of cell density in the white pulp at 2 days, lack of cells in the white pulp and absence of germinal centres for lymphoid follicles after 3 days.

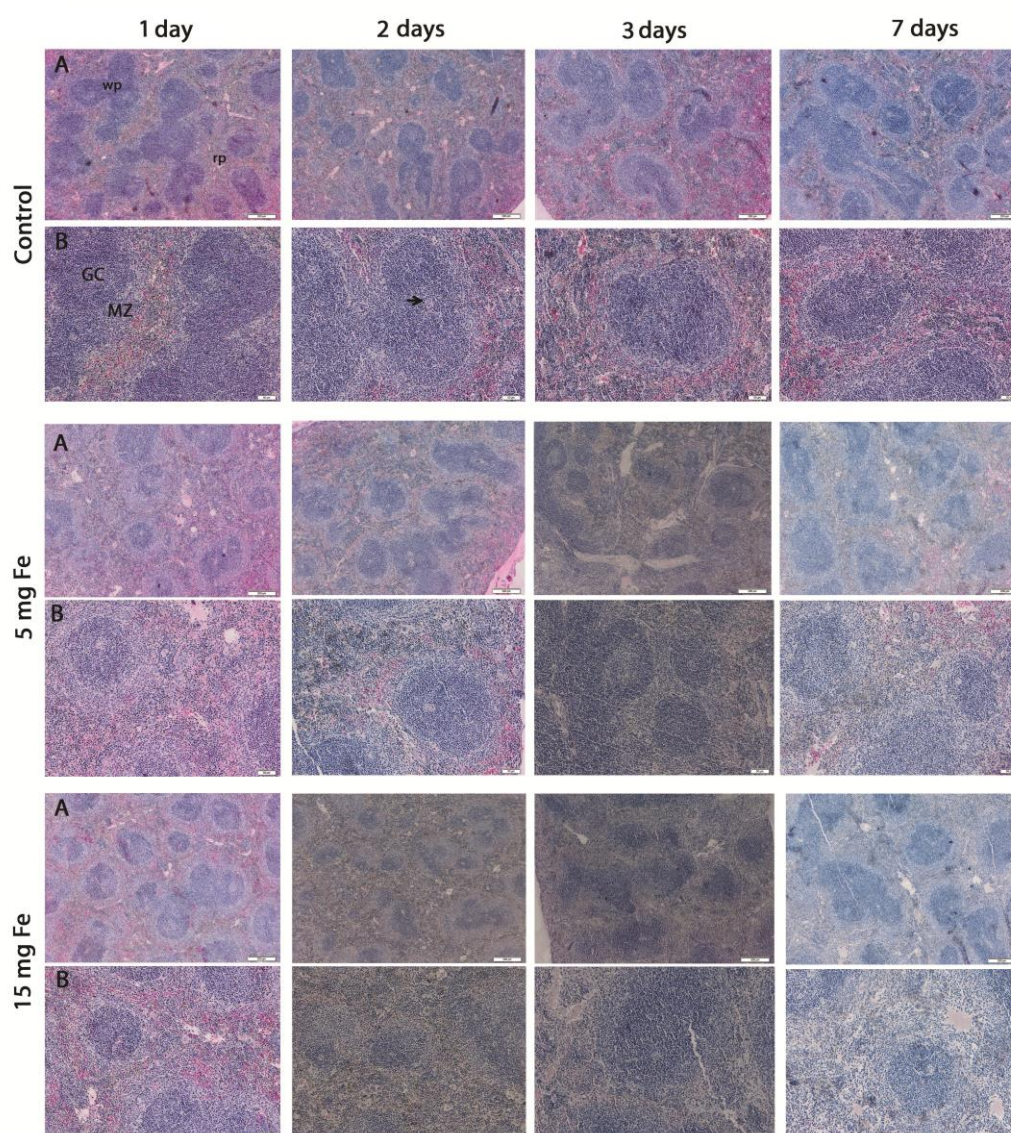


Figure 1. Histopathology of the spleen at 1, 2, 3 and 7 day post-exposure to 5 and 15 mg Fe/kg body weight DSPE-PEG micelles loaded with MNP; A. Scale bars: 200 μ m; B. Scale bars: 50 μ m; red pulp (RP), white pulp (WP), central arteriole (arrow), germinal centre (GC), marginal zone (MZ).

Prussian blue staining of the spleen sections showed stained areas of iron clumps in the red pulp, starting with control tissues and progressively enhanced from 1 to 3 days for experimental groups, especially for the highest iron dose (Figure 2). After the 7 days exposure, the Prussian blue-stained spleen sections for both nanoparticle groups appeared similar to the control. The maximum iron deposition after 3 days could be correlated with the structural changes observed in the histopathology analysis (Figure 2).

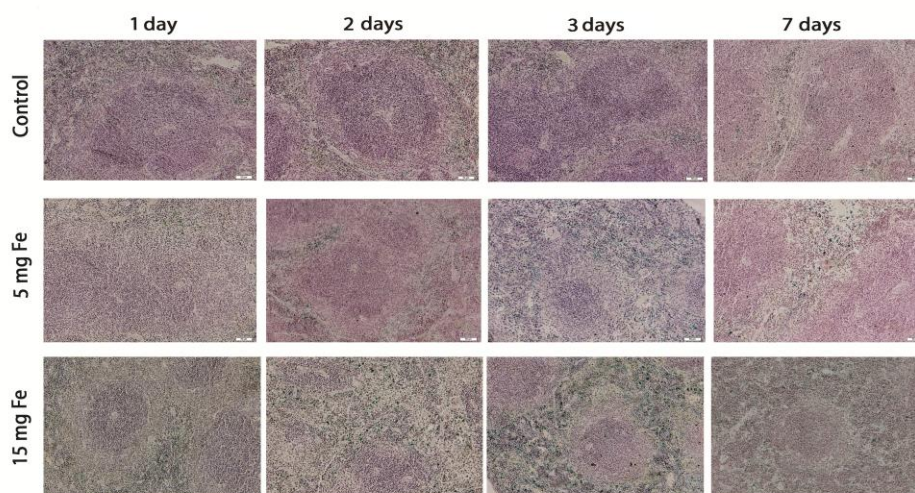


Figure 2. Prussian staining of the spleen at 1, 2, 3 and 7 days post-exposure to 5 and 15 mg Fe/kg body weight DSPE-PEG micelles loaded with MNP; iron nanoparticles – green.

Scale bars: 50 μ m.

3.3. Biochemical analyses

As shown in Figure 3, a significant increase in the MDA level, which was not dose related, was registered in the first day post-treatment by 26% and 28% for the 5 and 15 mg Fe/kg body weight dose, respectively, compared to control. By the second day, lower increases of 19% and 21% for the two doses were registered, compared to control. Also significant changes in MDA concentrations were observed after the third day, but after the 7 days exposure and up to 14 days one, MDA levels began to increase slightly in a non-significant manner.

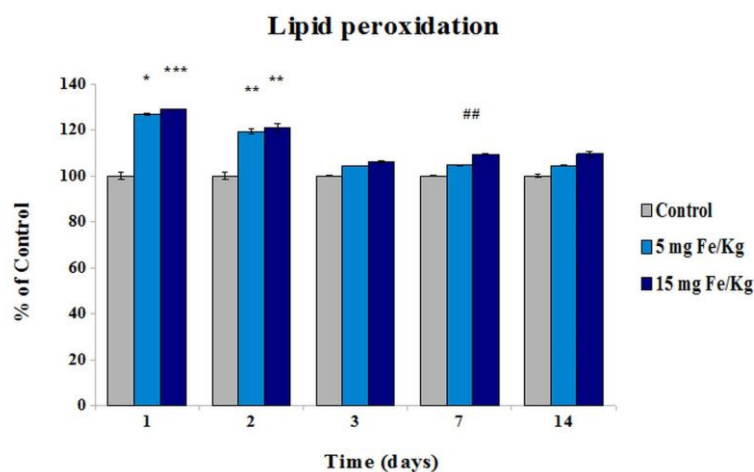


Figure 3. The progress of lipid peroxidation in control and exposed CD1 mice spleens (5 and 15 mg Fe/kg body weight concentrations of DSPE-PEG micelles loaded with MNP) for the indicated time intervals 1, 2, 3, 7 and 14 days. The values are represented as means \pm standard deviation (SD) ($n=7$ mice / subgroup: a control subgroup, a 5 mg Fe/kg body weight dose subgroup and a 15 mg Fe/kg body weight dose subgroup), expressed as % relative to control; * $p < 0.05$ the 5 and 15 mg Fe/kg body weight doses versus control groups; # $p < 0.05$ between the 5 mg Fe/kg body weight dose and the 15 mg Fe/kg body weight dose for each time interval

The GSH concentration, as illustrated in Figure 4, registered a significant increase 1 day

post-exposure, for both doses in comparison to control. The lower dose (5 mg Fe/kg body weight) generated a rise of 33% while the higher one (15 mg Fe/kg body weight) elicited an increase of 23%. After the third day of treatment, the GSH concentration significantly dropped below the control values by 13% and 16% for 5 mg Fe/kg and 15 mg Fe/kg body weight dose, respectively. In the next days, the GSH level gradually rose for the entire duration of the experiment, but remained below the level of control.

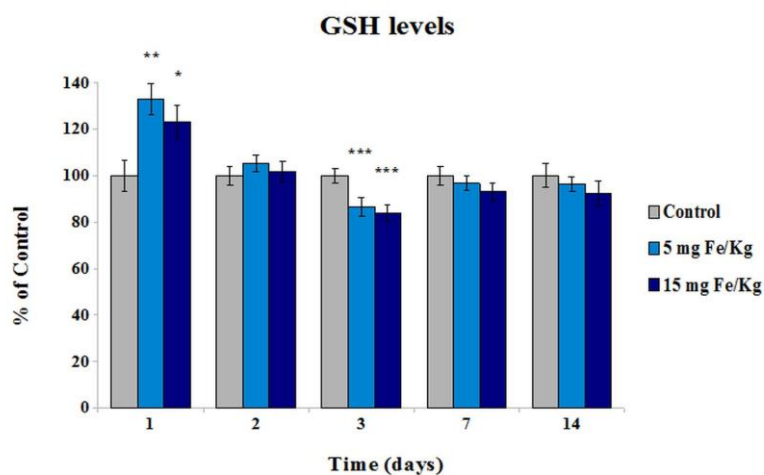


Figure 4. Effect of 5 and 15 mg Fe/kg body weight DSPE-PEG micelles loaded with MNP exposure on mice spleens GSH levels in time: 1, 2, 3, 7 and 14 days. Values are calculated as means \pm SD ($n=7$ mice / subgroup: a control subgroup, a 5 mg Fe/kg body weight dose subgroup and a 15 mg Fe/kg body weight dose subgroup) and expressed as % compared to control; * $p < 0.05$ the 5 and 15 mg Fe/kg body weight doses versus control groups

In our study, the AOPP levels increased in the first two days of exposure, but subsequently reverted to the control level for both doses (Figure 5). At 1 day post-exposure, increases by 33% (5 mg Fe/kg body weight dose) and 27% (15 mg Fe/kg body weight dose) compared to control were observed. After 3 days, the AOPP concentrations gradually decreased to values resembling control ones.

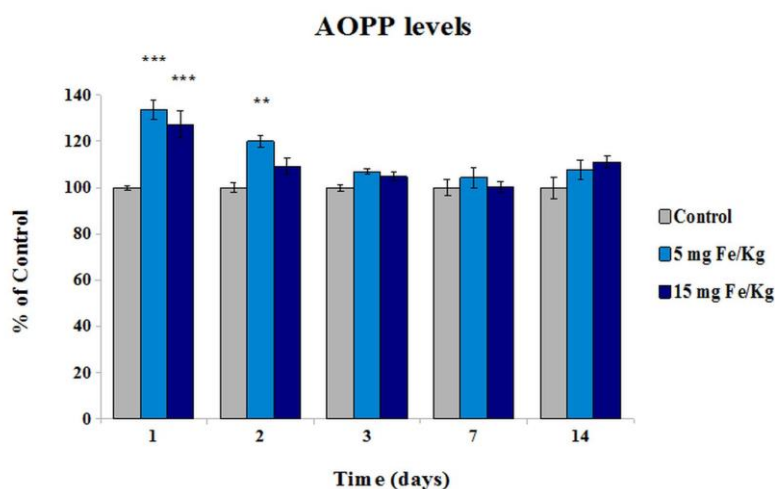


Figure 5. Time-dependent analysis of the advanced oxidation protein products in mice spleens exposed to 5 and 15 mg Fe/kg body weight DSPE-PEG micelles loaded with MNP

*and their progress, in a time (at 1, 2, 3, 7 and 14 days) and dose related manner. Values are expressed as means \pm SD (n=7 mice / subgroup: a control subgroup, a 5 mg Fe/kg body weight dose subgroup and a 15 mg Fe/kg body weight dose subgroup), percentage from the control; * $p < 0.05$ the 5 and 15 mg Fe/kg body weight doses versus controls*

4. Discussions

It is generally accepted that the coating of MNP used as contrast agents improves their biocompatibility and lowers their cytotoxicity. It was previously proved that polysaccharide dextran [22] or polyethylene glycol [23] fulfilled this desiderata. Our work was done in order to test the performance of modified phospholipid micelles loaded with MNP from the point of view of biocompatibility and potential toxicity.

In our experiment, the nanoparticles introduced by intravenous injection, were probably rapidly distributed within the body, where they were readily covered by serum proteins that act as opsonins, which facilitated the binding of the NP to phagocytic cells.

The liver, spleen and lymph nodes have high concentrations of phagocytic cells and as a result, the opsonized particles could be rapidly cleared from the circulation [24]. The coating of these NP with phospholipid polymeric micelles could reduce opsonization allowing them to remain in the circulation for much longer periods of time [25]. Furthermore, it would appear that while these 7 nm nanoparticles can't pass between the endothelial cells by the paracellular route, they can infiltrate the spleen endothelium which is discontinuous with larger fenestrations and lacking the basement membrane [24] possibly by transcytosis [26]. Alternatively, the macrophages from the red pulp of the spleen could take up the MNP by endocytosis, which could cause aggregation in clusters of different sizes [27]. Later on, the lysosomes of these cells might break down their iron oxide cores into iron ions [6], which could be eliminated or restored in the body through renal clearance, haemoglobin incorporation [28] or linked to different proteins like ferritin and transferrin [29].

In particular conditions, fractions of the nanoparticles could be retained in the body for long-term periods of time due to the uncompleted excretion and, consequently, may disturb the normal functions of organs and tissues by inducing toxicity in organs like the liver, spleen, lymph nodes and to a lesser extend the lungs [30].

The reduction of the white pulp follicles alongside the absence of germinal centres could indicate a significant level of immunosuppression as white pulp areas are sites of lymphocyte B maturation and the increase of iron content in the spleen could suggest 2 scenarios: either excess iron is stored in the red pulp because transferrin might already be saturated with iron and is not able to bind the excess or iron degradation products are deposited as a result of the phagocytosis of erythrocytes by macrophages in the red pulp [1,31].

The internalized MNP are probably degraded into Fe(II) ions within the lysosomes under the influence of hydrolysing enzymes which act at low pH [32]. The free Fe(II) ions react with hydrogen peroxide and produce hydroxyl radicals which are highly reactive and attack polyunsaturated fatty acids from biological membranes. As a result, the lipid peroxidation cascade occurs and breakdown products, such as MDA are formed. To our knowledge, this study is the first to investigate the oxidative modifications induced by MNP exposure in mice spleens. Previous research demonstrated that MDA levels were increased in a dose dependent manner in the liver and kidneys of Kumming mice exposed to MNP via intraperitoneal injection [33].

The increased iron accumulation could have generated an important oxidative stress and high GSH levels due to its raised synthesis in the first two days of exposure. Furthermore, increases in iron concentration in the spleen tissue could lead to an important reduction in GSH concentration as previously noticed for neuroblastoma cells [34].

AOPP, also markers of oxidative stress, are linked to the activation of phagocytes and act as inflammatory mediators [35]. They are formed by the myeloperoxidase-H₂O₂-halide system of activated phagocytes [36]. AOPP contain dityrosines resulted from the oxidation of the tyrosine residues, which allow for crosslinking and the formation of disulphide bridges and carbonyl groups [37].

In the spleen, the inducible hem oxygenase-1 is expressed five times more than

constitutive hem oxygenase-2 in order to catabolize the hem liberation from haemoglobin [38] and Fe^{2+} release [39]. When the iron concentration is high, it is stored predominantly in ferritin, a cytosolic protein comprised of 24 subunits of two types: H and L. In spleen cells, ferritin mostly contains L-subunits [40], specialized in iron storage [41]. When excess Fe^{2+} is released from MNP, the ROS formed during phagocytosis might determine an up-regulation of ferritin transcription [42]. This scenario could explain why starting with the third day of exposure the levels of MDA and AOPP decreased for the remaining duration of the experiment.

In addition, it has been previously reported that glutathione cycle enzymes are upregulated in the spleen of animals exposed to oxidant agents [43]. This could explain why the GSH concentration increased in the first 2 days of our study. The decrease of GSH levels in the third day could be due to the increase of glutathione-S-transferase activity, which is involved in cellular detoxification and utilizes this tripeptide as substrate. Glutathione depletion has been linked to chromatin structural alterations [44] and cell death [45]. In our case, the lack of cells in the white pulp after 3 day post-exposure could be due to the decreased concentration of glutathione. After 7 days, this tripeptide concentration returned to control levels and the structural damage were reduced.

5. Conclusions

As observed by histology analysis, following intravenous administration, the phospholipid polymeric micelles loaded with MNP progressively translocated to the spleen. The most significant changes were observed 3 days after exposure, when the most severe alterations, consisting of lack of cells in the white pulp and absence of germinal centres for lymphoid follicles, occurred. By contrast, for longer exposure periods, modifications were reduced. Also, the oxidative stress markers were transiently modified. Our data suggest that these phospholipid polymeric micelles loaded with MNP could be used as a contrast agent, but further deep investigations concerning their safety in clinical use are required.

Acknowledgements

To the POSDRU/159/1.5/S/133391 project, sustained by the European Social Fund, with gratitude for supporting this work.

References

- [1] M. Levy, N. Luciani, D. Alloyeau, D. Elgrabli, V. Deveaux, C. Pechoux, S. Chat, G. Wang, N. Vats, F. Gendron, C. Factor, S. Lotersztajn, A. Luciani, C. Wilhelm, F. Gazeau, *Biomaterials* **32**, 3988 (2011).
- [2] X. H. Peng, X. Qian, H. Mao, A. Wang, Z. Chen, S. Nie, D. Shin, *Int. J. Nanomedicine* **3**, 311 (2008).
- [3] J. Lodhia, G. Mandarano, N. J. Ferris, P. Eu, S. F. Cowell, *Biomed. Imaging Interv. J.* **6**: e12 (2010).
- [4] J. Wang, Y. Chen, B. Chen, J. Ding, G. Xia, C. Gao, J. Cheng, N. Jin, Y. Zhou, X. Li, M. Tang, X.M. Wang, *Int. J. Nanomedicine* **5**, 861 (2010).
- [5] A. Figuerola, R. Di Corato, L. Manna, T. Pellegrino, *Pharmacol. Res.* **62**, 126 (2010).
- [6] D. Thorek, A. Chen, J. Czupryna, A. Tsourkas, *Ann. Biomed. Eng.* **34**, 23 (2006).
- [7] R. Singh, J. W. Lillard, *Exp. Mol. Pathol.* **86**, 215 (2009).
- [8] A. J. Cole, A. E. David, J. Wang, C. J. Galbán, V. C. Yang, *Biomaterials* **32**, 6291 (2011).
- [9] Y. Chen, B.-A. Chen, *Chin. J. Cancer* **29**, 118 (2010).
- [10] C. J. Porter, S. M. Moghimi, L. Illum, S. S. Davis, *FEBS Lett.* **305**, 63 (1992).
- [11] J. Kreuter, *Adv. Drug Deliv. Rev.* **47**, 65 (2001).
- [12] K. Lind, M. Kresse, N. P. Debus, R. H. Müller, *J. Drug Target.* **10**, 221 (2002).

- [13] Y. Liu, K. Yang, L. Cheng, J. Zhu, X. Ma, H. Xu, Y. Li, L. Guo, H. Gu, Z. Liu, *Nanomedicine* **9**, 1077 (2013).
- [14] P. Couvreur, L. H. Reddy, S. Mangelot, J. H. Poupaert, S. Lepêtre-Mouelhi, B. Pili, C. Bourgaux, H. Amenitsch, M. Ollivon, *Small* **4**, 247 (2008).
- [15] P. Sharma, R. Dutta, A. Pandey, *Adv. Mater.* **2**, 246 (2011).
- [16] L. O. Cinteza, T. Y. Ohulchanskyy, Y. Sahoo, E. J. Bergey, R. K. Pandey, P. N. Prasad, *Mol. Pharm.* **3**, 415 (2006).
- [17] S. Sun, H. J. Zeng, *J. Am. Chem. Soc.* **124**, 8204 (2002).
- [18] O. H. Lowry, N. J. Rosebrough, A. L. Farr, R. J. Randall, *J. Biol. Chem.* **193**, 265 (1951).
- [19] D. Del Rio, N. Pellegrini, B. Colombi, M. Bianchi, M. Serafini, F. Torta, M. Tegoni, M. Musci, F. Brighenti, *Clin. Chem.* **49**, 690 (2003).
- [20] V. Witko-Sarsat, A. T. Nguyen, S. Descamp, B. Latsha, *J. Clin. Lab. Anal.* **6**, 47 (1992).
- [21] V. P. Torchilin, *J. Control. Release* **73**, 137 (2001).
- [22] D. Predoi, E. Andronescu, M. Radu, M. C. Munteanu, A. Dinischiotu, *Dig. J. Nanomater Bios* **5**(3), 779 (2010).
- [23] M. Yu, S. Huang, K. J. Yu, A. M. Clyne, *Int. J. Mol. Sci.* **13**, 5554 (2012).
- [24] M. C. Garnett, P. Kallinteri, *Occup. Med. (Lond.)* **56**, 307 (2006).
- [25] S. Stolnik, L. Illum, S. S. Davis, *Adv. Drug Deliv. Rev.* **16**, 195 (1995).
- [26] J. E. Schnitzer, *Adv. Drug Deliv. Rev.* **49**, 265 (2001).
- [27] L. Dai, Y. Liu, Z. Wang, F. Guo, D. Shi, B. Zhang, *Mater. Sci. Eng. C. Mater. Biol. Appl.* **41**, 161 (2014).
- [28] G. Mandarano, J. Lodhia, P. Eu, N. J. Ferris, R. Davidson, S. F. Cowell, *Biomed. Imaging Interv. J.* **6**: e13 (2010).
- [29] L. Gu, R. Fang, M. Sailor, J. H. Park, *ACS Nano*. **6**, 4947 (2012).
- [30] J. Li, X. Chang, X. Chen, Z. Gu, F. Zhao, Z. Chai, Y. Zhao, *Biotechnol. Adv.* **32**, 727 (2014).
- [31] A. Kunzmann, B. Andersson, T. Thurnherr, H. Krug, A. Scheynius, B. Fadeel, *Biochim. Biophys. Acta* **1810**, 361 (2011).
- [32] A. S. Arbab, L. B. Wilson, P. Ashari, E. K. Jordan, B. K. Lewis, J. A. Frank, *NMR Biomed.* **18**, 383 (2005).
- [33] P. Ma, Q. Luo, J. Chen, Y. Gan, J. Du, S. Ding, Z. Xi, X. Yang, *Int. J. Nanomedicine* **7**, 4809 (2012).
- [34] M. T. Nuñez, V. Gallardo, P. Muñoz, V. Tapia, A. Esparza, J. Salazar, H. Spelsky, *Free Radic. Biol. Med.* **37**, 953 (2004).
- [35] C. Capeillere-Blandin, V. Gausson, B. Descamps-Latscha, V. Witko-Sarsat, *Biochim. Biophys. Acta* **1689**, 91 (2004).
- [36] G. Marsche, S. Frank, A. Hrzenjak, M. Holzer, S. Dimberger, C. Wadsack, H. Scharnagl, T. Stojakovic, A. Heinemann, K. Oettl, *Circ. Res.* **104**, 750 (2009).
- [37] K. Šonka, L. Fialová, J. Volná, P. Jirontek, J. Vávrová, D. Kemlink, M. Prett, M. Kalousová, *Prague Med. Rep.* **109**, 159 (2008).
- [38] M. Knutson, M. Wessling-Resnick, *Crit. Rev. Biochem. Mol. Biol.* **38**, 61 (2003).
- [39] C. A. Schaer, G. Schoedon, A. Imhof, M. O. Kurrer, D. J. Schaer, *Circ. Res.* **99**, 943 (2006).
- [40] R. Invernizzi, M. Cazzola, P. De Fazio, V. Rosti, G. Ruggeri, P. Arosso, *Br. J. Haematol.* **76**, 427 (1990).
- [41] S. Levi, P. Santambrogio, A. Cozzi, E. Rovida, B. Corsi, E. Tamborini, S. Spada, A. Albertini, P. Arosio, *J. Mol. Biol.* **238**, 649 (1994).
- [42] Y. Tsuji, H. Ayaki, S. P. Whitman, C. S. Morrow, S. V. Torti, F. M. Torti, *Mol. Cell Biol.* **20**, 5818 (2000).
- [43] R. Ortiz-Butrón, V. Blas-Vaidivia, M. Franco-Colin, M. Pineda-Reynoso, E. Cano-Europa, *Drug Chem. Toxicol.* **34**, 180 (2011).
- [44] D. P. Evenson, L. K. Jost, J. Gandy, *Reprod. Toxicol.* **7**, 297 (1993).
- [45] F. Atroshi, A. Rizzo, I. Biese, P. Veijalainen, H. Saloniemi, S. Sankari, K. Andersson, *Pharmacol. Res.* **40**, 459 (1999).